

Some effects of galaxy structure and dynamics on the Fundamental Plane. II. A Virgo-Fornax distance modulus

Alister W. Graham^{*}

*Mount Stromlo and Siding Spring Observatories, The Australian National University,
Private Bag, Weston Creek PO, ACT 2611, Australia.*

ABSTRACT

The influence of broken structural homology, and the implied broken dynamical homology, is examined for the Fundamental Plane (FP). Requiring a symmetrical treatment of the FP variables, a bisector method of linear regression was applied, in 3-dimensions, to derive the best FP. A bootstrapping procedure has been used to estimate the uncertainties associated with the slope of the FP. For 25 E and S0 Virgo galaxies, the ‘standard’ FP, constructed using $R^{1/4}$ model parameters for the effective radii ($R_{e,4}$) and the mean surface brightness within this radius ($\Sigma_{e,4}$) and using central velocity dispersion (CVD) measurements (σ_0), gave a relation described by $R_{e,4} \propto \sigma_0^{1.10 \pm 0.14} \Sigma_{e,4}^{-0.55 \pm 0.09}$. Using Sersic $R^{1/n}$ light profile model parameters and the projected, infinite aperture, velocity dispersion ($\sigma_{\text{tot},n}$), derived from application of the Jeans equation to the observed intensity profiles, gave an ‘improved’ FP described by the relation $R_{e,n} \propto \sigma_{\text{tot},n}^{1.37 \pm 0.16} \Sigma_{e,n}^{-0.76 \pm 0.05}$. This result, based on independent data, supports the previous finding by Graham & Colless (1997a) that assumptions of structural and dynamical homology are partly responsible for the departure of the observed FP from the plane expected by the virial theorem, which predicts $R \propto \sigma^2 \Sigma^{-1}$. Upon removal of the known S0 galaxies from the sample of Virgo galaxies, the above planes were observed to change to $R_{e,4} \propto \sigma_0^{1.19 \pm 0.21} \Sigma_{e,4}^{-0.60 \pm 0.11}$ and $R_{e,n} \propto \sigma_{\text{tot},n}^{1.72 \pm 0.24} \Sigma_{e,n}^{-0.74 \pm 0.09}$. The perpendicular rms residuals about these planes are 0.084 and 0.050 dex, respectively.

The Fornax cluster was similarly treated, although removal of the S0 galaxies left a sample of only 7 ellipticals which had published CVD measurements. Treating the range of structural and dynamical profiles present in this sample produced a FP given by the relation $R_{e,n} \propto \sigma_{\text{tot},n}^{2.03 \pm 0.78} \Sigma_{e,n}^{-1.07 \pm 0.30}$, in tantalizing agreement with the plane expected from the virial theorem, but with discouragingly large errors due to the small sample size. Similarly to Virgo, the perpendicular rms residuals about this plane is 0.050 dex.

The FP was also constructed with the purpose of using it as a distance indicator, achieved by minimising the distance-dependent quantity $\log R$ against the distance-independent quantities Σ and $\log \sigma$. A Virgo-Fornax distance modulus was computed using Working-Hotelling confidence bands (Feigelson & Babu 1992). The ‘standard’ FP parameters gave a value of 0.45 ± 0.16 mag, where-as the ‘improved’ FP parameters gave a value of 0.25 ± 0.12 mag. However, a full treatment of the uncertainties on the FP slopes, derived through a bootstrapping procedure of the 3-dimensional FP data set, revealed that the analytical expressions for the uncertainties on the estimated distance moduli, given above, should be increased by a factor of ~ 5 .

Key words: galaxies: fundamental parameters – galaxies: structure – galaxies: kinematics and dynamics. galaxies: elliptical and lenticular, cD – distance scale

1 INTRODUCTION

Our knowledge about the structure of elliptical galaxies has progressed considerably in the last decade. No longer are

^{*} E-mail: ali@mso.anu.edu.au

we satisfied with fitting a de Vaucouleurs (1948,1953) $R^{1/4}$ intensity distribution to the light profiles of elliptical galaxies. Modern imaging techniques are providing ever-more precise measurements, revealing a range of light profile shapes which have been shown to be better described by the Sersic (1968) $R^{1/n}$ model (Capaccioli 1989; Caon, Capaccioli & D’Onofrio 1993; Graham et al. 1996, and references within). Through varying the parameter n in the Sersic model, one can reproduce an exponential light distribution ($n=1$), the classic de Vaucouleurs profile ($n=4$), approximate a power-law for large values of n (approximately >15), or any of the intermediate forms which galaxies exhibit (Michard 1985; Schombert 1986; Binggeli & Cameron 1991; Caon et al. 1993; Graham & Colless 1997a, hereafter Paper I, to mention a few). Consequently, for those galaxies which are not well described by an $R^{1/4}$ profile, the effective radius and mean surface brightness within this radius will be different when obtained using the de Vaucouleurs model and the Sersic model. More importantly, these differences have been shown to have a systematic trend: galaxies with $n < 4$ have their effective half-light radii over-estimated by the $R^{1/4}$ model, and galaxies better described with values of $n > 4$ have their effective half-light radii under-estimated by the $R^{1/4}$ model. Similarly, the mean surface brightness is under- and over-estimated by the $R^{1/4}$ model when $n < 4$ and $n > 4$ respectively (Graham & Colless 1997b).

Observed variations in the galaxy structure, as described by the $R^{1/n}$ model, imply a variety of dynamical structures (Ciotti 1991; Paper I) are required to maintain these predominantly pressure-supported stellar systems. This conjecture is borne out in the observations of elliptical galaxy dynamics (Davies et al. 1983; Illingworth 1983; Capaccioli & Longo 1994) and has implications for the construction of the Fundamental Plane (FP). In particular, the use of a galaxy’s central velocity dispersion (CVD, σ_0) to represent the overall kinetic energy of a galaxy has been shown to be inappropriate, (Jørgensen, Franx & Kjørgaard 1993; Bender, Saglia & Gerhard 1994). The velocity dispersion derived from the kinetic energy of random motion over the entire galaxy surface has been shown to be proportional to $\sigma_0^{1.6}$ rather than σ_0^2 (Busarello et al. 1997). A procedure is described in Paper I, based upon the theoretical study of Ciotti (1991), which enables the velocity dispersion to be measured in a consistent fashion between galaxies. Rather than simply using CVD measurements, that sample different fractions of different galaxies’ velocity dispersion profiles (in terms of the half-light radii), through application of the Jeans equation, Paper I presented a method to compute the asymptotic value of the velocity dispersion within a projected aperture of infinite radius. This measure, denoted by σ_{tot} , has the added significance of being equal to one-third of the virial velocity for spherical systems (Ciotti 1994).

In Paper I the light profile data (aperture magnitudes from Bower, Lucey & Ellis 1992) from a sample of 26 E/S0 Virgo galaxies was analysed. Departures from the $R^{1/4}$ model were found to be well-described by the Sersic model, and the implied non-homology in the velocity dispersion profile was explored. Using the Sersic model parameters, rather than $R^{1/4}$ model parameters, and using the computed, infinite aperture velocity dispersion rather than the CVD, the FP was observed to change from $R_{e,4} \propto \sigma_0^{1.33 \pm 0.10} \Sigma_{e,4}^{-0.79 \pm 0.11}$ to $R_{e,n} \propto \sigma_{tot,n}^{1.44 \pm 0.11} \Sigma_{e,n}^{-0.93 \pm 0.08}$. Broken structural and dy-

namical homology appeared to be responsible for some of the *tilt* of the FP, i.e. its departure from the plane predicted by the virial theorem, $R \propto \sigma^2 \Sigma^{-1}$.

Ultimately, this broken dynamical and structural homology needs to be dealt with if one is to understand the nature of elliptical galaxies and use them for measuring distances (Dressler et al. 1987). Given the substantial improvements in describing elliptical galaxies, it is apt that the FP, and its application to distance estimates, is revisited. Using a new data base (taken from Caon et al. 1994) obtained by different observers with a different instrument and using a different reduction procedure, the influence of broken structural and broken dynamical homology upon the FP is again investigated. The data used in this paper is the surface brightness profiles along the major axis of each galaxy, as opposed to the integrated aperture magnitudes used in Paper I. The influence of S0 galaxies upon the slope of the FP is also investigated, with comparison of the FPs constructed with, and without, their inclusion.

This paper presents the FP for the galaxy clusters Fornax and Virgo, two key clusters in the extra-galactic distance scale (Jacoby et al. 1992; McMillan, Ciardullo & Jacoby 1993; Bureau, Mould & Staveley-Smith 1996). These clusters are sufficiently distant to possess significant motion due to the Hubble expansion and yet they are close enough that their distances may be obtained with a plethora of independent observational techniques. The following section presents the galaxy sample and the observational/model data which is used in this study. The Fundamental Plane is computed, and its method of construction, including a new error analysis routine, is described in Section 3. Using two different methods of analysis, a distance modulus between Virgo and Fornax is calculated in Section 4. This result is compared with other estimates of the Virgo-Fornax distance modulus in Section 5, along with a discussion of the other results. Section 6 provides a summary and concluding remarks.

2 GALAXY DATA

2.1 The galaxy sample

The galaxy sample from Caon et al. (1994) has been used for this investigation. This data set has been used in a benchmark study (Caon et al. 1993) which gave insight into the nature of elliptical galaxy light profiles by quantifying their deviations from the $R^{1/4}$ model. Knowing that this galaxy sample does not possess structural homology amongst its members makes it an ideal sample to explore the necessarily implied broken dynamical homology and the combined influence of these effects upon the FP. From the sub-sample of galaxies for which major-axis profiles have been modeled (see Caon et al. 1993 for a discussion of some of the problems in doing this), those which have no published velocity dispersion data have been excluded here. This reduced the sample of Virgo galaxies from 33 (Caon et al. 1993) to 25, and the sample of Fornax galaxies from 16 (D’Onofrio, Capaccioli & Caon 1994) to 10. The 10 Fornax galaxies were further reduced to a sample of 9 after the exclusion of NGC 1399, which, with its shallow light profile ($n > 15$), could not have its velocity dispersion profile accurately modeled due

to the large uncertainties associated with the effective radius R_e . The remaining galaxies are listed in Table 1.

2.2 Surface brightness profiles and structural model parameters

The B band surface brightness profiles from Caon et al. (1994) have been used in this study. They were constructed by these authors using the ‘global mapping’ procedure of Capaccioli & Caon (1989) which couples CCD data for the bright inner galaxy profile with photographic data for the outer profile. This technique allows very deep photometry of galaxies, and alleviates the problem of uncertain sky subtraction errors that is associated with the use of small area CCD’s. The method gives internal errors of less than 0.1 mag at $\mu_B=26$ mag.

In this study the major-axis surface brightness profiles have been truncated at the same inner and outer limits that were applied by Caon et al. (1993) and D’Onofrio et al. (1994) for the Virgo and Fornax galaxies respectively. In general, this meant fitting the entire light profile after the exclusion of the inner portion affected by seeing, and the outer portion where sky subtraction uncertainties became large (>0.25 mag). This left a typical range in surface brightness from $\mu_B=20$ to 27 mag.

The Sersic (1968) $R^{1/n}$ light profile model was fitted to the remaining profile, with the intensity I given as a function of radius R such that

$$I(R) = I_e \exp \left[-b(n) \left[\left(\frac{R}{R_e} \right)^{1/n} - 1 \right] \right]. \quad (1)$$

I_e is the intensity at the radius R_e , and $b(n)$ ($\approx 1.9992n - 0.3271$, Capaccioli 1989) is defined such that R_e is the radius that effectively encloses half of the total light of the profile model (Caon et al. 1993; Graham & Colless 1996). The ‘shape parameter’ n describes the curvature of each light profile. Application of a non-linear least-squares fit of the $R^{1/n}$ model to the galaxy surface brightness data, with equal weight for each data point, produced similar values for the shape parameters to those derived by Caon et al. (1993) and D’Onofrio et al. (1994), confirming that the models are being fitted consistently between authors.

Table 1 lists the parameters from the best fitting $R^{1/n}$ model and also those from the best fitting $R^{1/4}$ model, which was fitted in an identical fashion. Σ_e is the mean surface brightness within the effective radius R_e , computed using the technique described in Appendix A of Paper I. The subscripts n and 4 on the model parameters are used to denote the model from which the particular parameters have come; n signifying $R^{1/n}$ model parameters, and 4 signifying $R^{1/4}$ model parameters.

Ciotti (1991), and also Paper I, explored the relationship between the projected and spatial (deprojected) quantities. By definition, the surface brightness terms had a one-to-one mapping, while there was an approximately constant offset ($\log R \sim 0.13$, Ciotti 1991) between the effective radii. Therefore either of these quantities could be used for the construction of the FP. The deprojected velocity dispersion at the effective radius was found not to have such a simple relation with its projected counterpart, the central velocity dispersion measurement. This deprojected velocity dis-

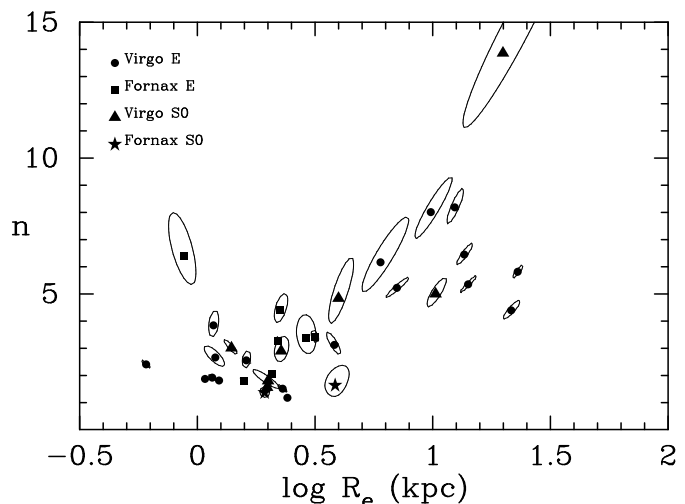


Figure 1. The shape parameter n is plotted against the $R^{1/n}$ model effective radius R_e for the Virgo and Fornax galaxies listed in Table 1. The associated 99% confidence interval is also drawn, as detailed in the text.

person is preferred over the CVD measurement because it not only allows for the range of velocity dispersion profiles present, but also samples different galaxies in a consistent fashion (CVD measurements sample typically anywhere between $0.01-0.2 R_e$). However, due to the physical significance of the projected velocity dispersion within an aperture of infinite radius, this term, which also samples different galaxies in a consistent fashion, is preferred in the analysis which follows.

Following Caon et al. (1993) (their Fig. 3), the light profile shape parameter is plotted against galaxy scale-size in Figure 1. Although our methods of parameterisation differ (Caon et al. 1993 have used model-independent estimates for the half-light radius), the same trend of increasing values of n with R_e is evident here. The present study also includes Fornax galaxies as well as those from Virgo. Also shown in the figure are the 99% confidence intervals for the model parameters. These were computed by evaluating the chi-square values for a fine grid of points around the optimum solution. The contours drawn correspond to $\Delta\chi^2=9.21$ (i.e. 4σ), scaled after normalisation of the reduced χ^2 of the optimum solution. [†]

In exploring the sensitivity of the $R^{1/n}$ model parameters to the radial range of the surface brightness profile, the Sersic model was fitted to that data within the inner $40''$. This outer truncation is the same as the outermost data points used in Paper I, enabling a further comparison of the present data with that used in Paper I. The inner truncation used by Caon et al. (1993) and D’Onofrio et al. (1994) was again employed, except for NGC 4473 and NGC 4636 for which only the inner $3''$ was excluded. In Figure 2, the resulting model parameters are shown plotted against those obtained using the entire surface brightness profile (Table

[†] It is noted that these confidence intervals only encompass the uncertainty of the parameters derived from the analytical fit to the data. They do not incorporate measurement errors or zero point offsets which may be present in the data.

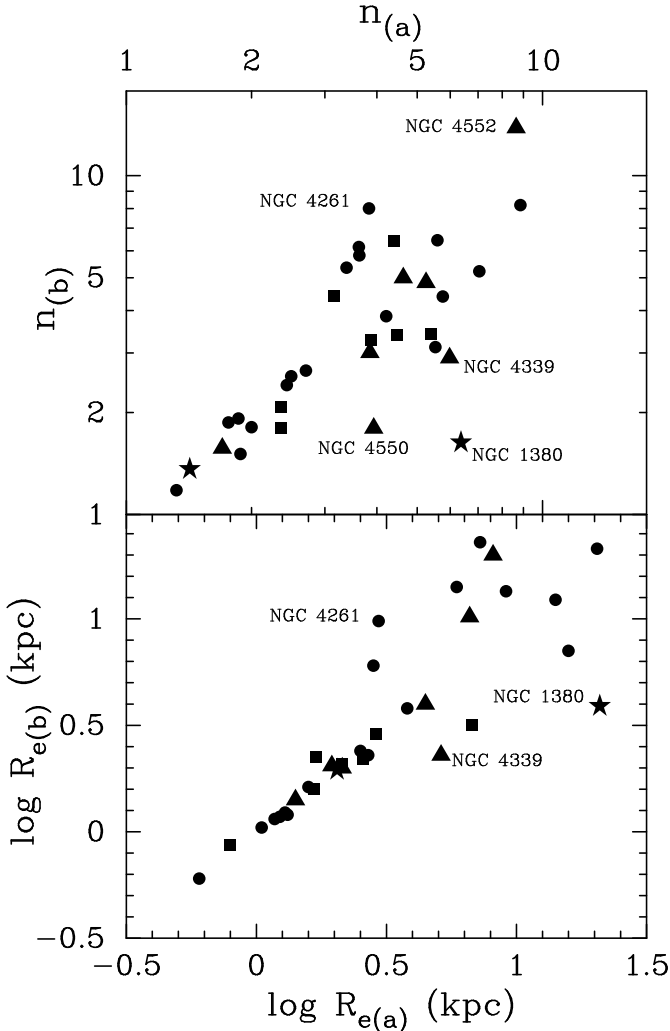


Figure 2. The Sersic $R^{1/n}$ model parameters from the fit to the entire light profile (subscript b) are plotted against those parameters obtained from fit to the light profile within $40''$ (subscript a). The circles represent Virgo E's (18), the triangles are Virgo S0's (7), the squares are Fornax E's (7) and the stars represent Fornax S0's (2).

1). It is noted that the light profiles from the smaller radial extension ($<40''$) may not be representative of the galaxy as a whole, and therefore may not represent the *over-all* global galaxy shape. This is more likely to be true for the larger galaxies, especially those having $R_e > 40''$. It is also true that the Sersic index n is less sensitive at larger values (Graham et al. 1996). Thus, Figure 2 offers an alternative estimate for the uncertainty of the $R^{1/n}$ model parameters. Some of the more discrepant points have been labeled in the plot. It is noted that they are predominantly the S0 galaxies. If one is to think of these galaxies as possessing an $R^{1/4}$ ($n=4$) central bulge and an exponential ($n=1$) outer disk, or some approximately equivalent Sersic form, then this could account for the larger index obtained using the smaller radial range for the S0 galaxies NGC 1380, 4339, and 4550. In fact, such measurements offer themselves as possible diagnostics for distinguishing S0 galaxies from ellipticals.

For the Fornax galaxies, the tabulated extinctions range from $A_B = -0.05$ to -0.09 . Some of the Virgo galaxies also

have negative extinctions, with a mean Virgo cluster value of $A_B = 0.04 \pm 0.07$ (standard deviation) for the sample. The negative values are due to the variable ratio of H_I gas-to-dust in the Galaxy (Burstein & Heiles 1978), and have no physical meaning. Such values arise in the method used by Burstein & Heiles for regions where there is zero or negligible reddening, and they should be set equal to 0.00. Corrections for Galactic extinction (Burstein & Heiles 1984; Burstein et al. 1987) were not applied by Caon et al. (1994). This practice has been maintained here.

At a redshift of around 0.003, the k-correction and redshift dimming will be equally small for both clusters, at 0.015 mag and 0.013 respectively. Consequently these terms have not been incorporated into the analysis.

2.3 Dynamical model parameters

CVDs are typically used as a measure of the kinetic energy within elliptical and S0 galaxies. There are many problems associated with doing this. Firstly, rotational energies, which are likely to be significant for S0 galaxies, are ignored. Secondly, fixed aperture sizes (on the sky) in which the CVD is measured correspond to different physical sizes for galaxies in clusters at different distances. This effect alone may likely introduce systematic errors into cluster distance determinations which have incorporated fixed aperture sizes to measure the CVD. Thirdly, given that galaxies have a range of sizes and structural profiles, they will also have a range of dynamical profiles which support the various structures that are observed. Therefore, even within clusters, fixed aperture sizes will sample different fractions of individual galaxies, as measured in terms of their effective radii.

In an attempt to find a better measure of the kinetic energy within each galaxy, a method of computing the velocity dispersion in a consistent manner for all galaxies was presented in Paper I. Deprojecting the galaxy light profile, the spatial luminosity density (Ciotti 1991) was computed. Assuming a constant M/L ratio within each galaxy, such knowledge of the internal density profile coupled with the application of the Jeans hydrodynamical equation enables one to compute the internal velocity dispersion profile. This can then be projected outward to give the projected radial velocity dispersion profile, which in turn can be integrated over increasing aperture sizes to give the projected aperture velocity dispersion profile. This is then calibrated using the measured CVD.

The computed spatial (deprojected) velocity dispersion at the spatial half-light radius was used in Paper I to represent the kinetic energy of the galaxies. Unlike use of CVD, this approach consistently samples the velocity dispersion profile in the same way for all galaxies. As an alternative, the computed velocity dispersion within an aperture of infinite radius was also used. This quantity has been shown by Ciotti (1994) to be equal to one-third of the virial velocity dispersion, independent of any orbital anisotropies that may be present. This measure for the kinetic energy is adopted here, not only for the consistent fashion in which galaxies are sampled but also due to the significance of the infinite aperture velocity dispersion σ_{tot} . These values are listed in Table 1, where the subscripts 4 and n refer to use of the $R^{1/4}$ and $R^{1/n}$ models respectively. Also listed are the CVD measurements, σ_0 , from McElroy (1995).

Table 1. Galaxy model parameters. The galaxy sample is a selection from Caon et al. (1994). The parameters are from the best fitting $R^{1/4}$ and $R^{1/n}$ models, with the exception of σ_0 which is the tabulated central velocity dispersion from McElroy (1995). $R_{e,4}$ and $R_{e,n}$ are the effective radii of the $R^{1/4}$ and the $R^{1/n}$ models respectively, with $\Sigma_{e,4}$ and $\Sigma_{e,n}$ the mean surface brightness within R_e . $\sigma_{\text{tot},4}$ and $\sigma_{\text{tot},n}$ are the infinite aperture velocity dispersions described in the text.

Galaxy Ident.	Morph. Type	σ_0 km s ⁻¹	n	log $R_{e,n}$ [kpc]	$\Sigma_{e,n}$ [mag]	$\sigma_{\text{tot},n}$ km s ⁻¹	log $R_{e,4}$ [kpc]	$\Sigma_{e,4}$ [mag]	$\sigma_{\text{tot},4}$ km s ⁻¹
NGC 1339	E4	160	1.80	0.20	20.78	138	0.04	19.74	134
NGC 1351	E5	143	3.38	0.46	21.52	112	0.46	21.46	110
NGC 1374	E0	186	3.28	0.34	20.93	149	0.32	20.77	147
NGC 1375	S0	53	1.36	0.29	21.27	53	0.40	21.59	41
NGC 1379	E0	119	2.07	0.32	20.96	100	0.26	20.57	95
NGC 1380	S0/a	225	1.63	0.59	20.61	191	0.72	21.01	166
NGC 1404	E2	250	4.42	0.35	19.82	193	0.34	19.79	196
NGC 1419	E0	133	6.41	-0.06	20.35	110	0.02	20.89	112
NGC 1427	E4	155	3.42	0.50	21.36	121	0.49	21.27	118
NGC 4168	E2	186	6.16	0.78	22.82	125	0.64	22.35	139
NGC 4261	E2	326	8.01	0.99	22.82	196	0.74	21.91	240
NGC 4339	S0(0)	114	2.90	0.36	21.48	92	0.38	21.54	89
NGC 4365	E3	261	6.45	1.13	22.83	164	0.96	22.14	190
NGC 4374	E1	296	8.19	1.09	22.33	173	0.91	21.69	216
NGC 4387	E5	112	1.92	0.06	20.35	99	0.00	19.89	95
NGC 4431	dS0,N	68	1.57	0.30	22.29	58	0.60	23.50	51
NGC 4434	E0	115	3.85	0.07	20.63	96	0.07	20.63	96
NGC 4458	E1	106	2.56	0.21	21.30	89	0.24	21.29	85
NGC 4459	S0(2)	178	4.84	0.60	21.20	130	0.57	21.14	134
NGC 4464	E3	121	2.41	-0.22	19.48	111	-0.38	18.44	112
NGC 4472	E2	303	5.82	1.36	22.74	193	1.21	22.15	221
NGC 4473	E5	193	3.12	0.58	20.88	151	0.53	20.51	146
NGC 4476	S0(5)	81	3.01	0.15	20.77	68	0.06	20.19	68
NGC 4478	E2	143	1.87	0.03	19.70	127	-0.10	18.92	124
NGC 4486	E0	333	5.35	1.15	22.29	221	1.01	21.78	242
NGC 4550	S0(7)	83	1.80	0.30	20.25	71	0.01	18.38	70
NGC 4551	E2	113	1.81	0.09	20.56	99	-0.03	19.90	96
NGC 4552	S0(0) ^a	269	13.86	1.30	23.73	117	0.76	21.60	198
NGC 4564	E6	160	1.51	0.36	20.59	137	0.07	18.63	133
NGC 4621	E4	230	5.22	0.85	21.61	159	0.70	21.05	170
NGC 4623	E7	89	1.18	0.38	21.41	89	0.30	20.71	70
NGC 4636	E1	207	4.40	1.33	23.43	147	1.30	23.29	152
NGC 4649	S0(2)	339	5.00	1.01	21.70	232	0.95	21.48	247
NGC 4660	E3	185	2.66	0.08	19.39	159	-0.03	18.78	158

^a Also known as M 89, this galaxy is catalogued as type E in de Vaucouleurs et al. (1991).

3 CONSTRUCTION OF THE FUNDAMENTAL PLANE

The quantities which are used in this investigation of the FP are the effective radius, R_e , and the mean surface brightness within this radius, Σ_e , derived from the model fits to the surface brightness profiles. These values are listed in Table 1. This approach differs from D’Onofrio, Longo & Capaccioli (1996), who used model-independent values for these quantities in their construction of the FP. They also only used CVDs for their velocity dispersion measure.

In this section, the Fundamental Plane is constructed with the goal of comparison with theoretical predictions. Consequently, the 3 parameters which are used to define the FP (σ, R, Σ) are treated as independent of each other. This requires a symmetrical treatment of these parameters, and

the bisector method of linear regression is the preferred technique (Isobe et al. 1990; Feigelson & Babu 1992). This approach requires that three FPs be computed, each of which is obtained by minimising the residuals of a different parameter. The mean slope angles of these 3 planes are then used to represent the final FP.

The uncertainties associated with the FP slope are also important. Feigelson & Babu (1992) not only show that the standard formula (e.g. Bevington 1969) for calculating the uncertainties on the derived slope and intercept is in general mathematically incorrect, but they also show that the derived asymptotic, analytic expressions for the variance will under-estimate the true variance when the sample size is small (approximately ≤ 50). They therefore recommend the use of a bootstrapping procedure to gauge the variance on the fitted slope and its intercept. This approach was followed

Table 2. Fundamental Plane $R\propto\sigma^A\Sigma^B$ for a sample of 25 E & S0 Virgo galaxies constructed using the bisector method of linear regression in 3 dimensions. The errors are from a bootstrapping procedure. The approach referred to as $R^{1/4}[\sigma_0]$ has used the effective radius from the $R^{1/4}$ model, the mean surface-brightness within this radius, and the projected CVD, σ_0 , in the construction of the FP. $R^{1/n}[\sigma_{\text{tot},n}]$ uses the infinite aperture velocity dispersion term, $\sigma_{\text{tot},n}$, and the effective radius and associated surface brightness term from the $R^{1/n}$ model.

model	$R\propto\sigma^A\Sigma^B$		\perp rms residual
	A	B	
$R^{1/4}, \sigma_0$	1.10±0.14	-0.55±0.09	0.099
$R^{1/n}, \sigma_0$	1.12±0.17	-0.64±0.07	0.084
$R^{1/4}, \sigma_{\text{tot},4}$	1.17±0.15	-0.60±0.08	0.100
$R^{1/n}, \sigma_{\text{tot},n}$	1.37±0.16	-0.76±0.05	0.077

Table 3. Fundamental Plane $R\propto\sigma^A\Sigma^B$ for a sample of 18 E Virgo galaxies constructed using the bisector method of linear regression in 3 dimensions. The errors are from a bootstrapping procedure.

model	$R\propto\sigma^A\Sigma^B$		\perp rms residual
	A	B	
$R^{1/4}, \sigma_0$	1.19±0.21	-0.60±0.11	0.084
$R^{1/n}, \sigma_0$	1.22±0.25	-0.66±0.12	0.071
$R^{1/4}, \sigma_{\text{tot},4}$	1.28±0.24	-0.65±0.11	0.085
$R^{1/n}, \sigma_{\text{tot},n}$	1.72±0.24	-0.74±0.09	0.050

in this study. However, this numerical resampling technique was modified for application to the small sample of Fornax elliptical galaxies in order to exclude 10% of the 400 bootstrapping simulations with a negative, rather than positive, slope. These simulations were excluded from the computation of the final slope variance due to their obviously wild departure from the expected value. Such FP's are due to the small sample size of 7 points in Fornax. With the somewhat larger sample of Virgo galaxies (25) this problem did not arise in any of the 2000 simulations used.

The total sample of Virgo galaxies contains 18 E's and 7 S0's. It was therefore possible to compute the FP using both the entire sample, and using only elliptical galaxies. In addition, given the four sets of FP parameters ($\log \sigma_0, \log R_{e,4}, \Sigma_{e,4}$), ($\log \sigma_0, \log R_{e,n}, \Sigma_{e,n}$), ($\log \sigma_{\text{tot},4}, \log R_{e,4}, \Sigma_{e,4}$) and ($\log \sigma_{\text{tot},n}, \log R_{e,n}, \Sigma_{e,n}$), a total of eight FP's have been computed for the Virgo cluster. The results are shown in Table 2 and Table 3, where the rms residual is that perpendicular to the fitted plane. The uncertainties on the estimated slopes are those from the bootstrapping procedure, and are therefore larger than the standard analytically determined uncertainties derived for the FP. Using the sample of 7 available Fornax elliptical galaxies an additional four planes were computed using the above mentioned four sets of parameters. Table 4 shows the results.

A Principal Component Analysis (PCA) was performed on each of the four 3 dimensional data sets from the combined E & S0 Virgo galaxy sample. The code from Murtagh & Heck (1987) was implemented to show the degree to which

Table 4. Fundamental Plane $R\propto\sigma^A\Sigma^B$ for a sample of 7 E Fornax galaxies constructed using the bisector method of linear regression in 3 dimensions. The errors are from a bootstrapping procedure.

model	$R\propto\sigma^A\Sigma^B$		\perp rms residual
	A	B	
$R^{1/4}, \sigma_0$	1.69±0.83	-0.85±0.30	0.064
$R^{1/n}, \sigma_0$	1.79±0.79	-0.98±0.28	0.049
$R^{1/4}, \sigma_{\text{tot},4}$	1.85±0.86	-1.00±0.35	0.070
$R^{1/n}, \sigma_{\text{tot},n}$	2.03±0.78	-1.07±0.30	0.050

Table 5. Fractional Variance from the Principal Component Analysis on the sample of 25 Virgo E & S0 galaxies.

model	Var ₁	Var ₂	Var ₃
$R^{1/4}, \sigma_0$	76.03%	21.99%	1.98%
$R^{1/n}, \sigma_0$	82.79%	15.80%	1.41%
$R^{1/4}, \sigma_{\text{tot},4}$	72.30%	25.57%	2.13%
$R^{1/n}, \sigma_{\text{tot},n}$	75.18%	23.44%	1.38%

the data sets are defined by a 2-dimensional plane within the 3-space of observables. Table 5 displays the fractional variance of the data along the major eigenvectors of the FP parameter space. This reveals that greater than 97% of the variance in the data indeed lies in a plane, confirming the appropriateness of constructing a plane to describe the properties of elliptical galaxies.

4 THE VIRGO-FORNAX DISTANCE-MODULUS

Only the elliptical galaxy population is used in the following determination of the Virgo-Fornax distance-modulus due to the contaminating influence of the S0 galaxies on the FP. Contaminating in the sense that S0 galaxies may possess a significant degree of rotational energy which is ignored in the present analysis.

The problem of computing the offset between two parallel data sets, with an emphasis on cosmic distance scale calibrations, is well described in Isobe et al. (1990) and Feigelson & Babu (1992). If the objective in constructing the FP is for the purpose of computing distances between galaxy clusters, then the FP parameters should be treated differently than they were treated in Section 3 (where the FP was constructed for comparison with a theoretical prediction). In this case, one wishes to predict the value of a distance-dependent quantity, namely $\log R$, from the distance-independent quantities $\log \sigma$ and Σ . Consequently, the plane that is fitted to the data should be computed through an ordinary least-squares minimisation of the distance-dependent quantity, rather than using the bisector method of linear regression which treats all variables equally (Section 3). This approach will minimise the uncertainty on the estimate of the relative distance between clusters. Such an approach was taken with the two extreme Virgo and Fornax data sets, ($\log \sigma_0, \log R_{e,4}, \Sigma_{e,4}$) and ($\log \sigma_{\text{tot},n}, \log R_{e,n}, \Sigma_{e,n}$). (These are extreme in the sense of

Table 6. Fundamental Plane $R \propto \sigma^A \Sigma^B$ using only elliptical galaxies. Constructed using ordinary linear regression, in 3-dimensions, that minimised the $\log R$ residuals. The errors are from a bootstrapping procedure.

model	$R \propto \sigma^A \Sigma^B$		(log R) rms residual
	A	B	
Virgo: $R^{1/4}, \sigma_0$	1.11±0.27	-0.59±0.13	0.134
Fornax: $R^{1/4}, \sigma_0$	1.14±0.84	-0.59±0.29	0.120
Virgo: $R^{1/n}, \sigma_{\text{tot},n}$	1.62±0.27	-0.74±0.12	0.100
Fornax: $R^{1/n}, \sigma_{\text{tot},n}$	1.47±0.82	-0.81±0.34	0.110

Table 8. Distance moduli given by $5(\Delta \log R)$, where $\Delta \log R$ is the computed intercept offset between the cluster FPs, as described in the text. These have been obtained using a generalisation of the Working-Hotelling confidence bands (Feigelson & Babu 1992), using both Virgo and Fornax as the calibration sample. The uncertainties are from the asymptotic formula fits given in Table 7.

Calibrator sample	$R^{1/4}[\sigma_0]$ mag. offset	$R^{1/n}[\sigma_{\text{tot},n}]$ mag. offset
Virgo:	-0.46±0.23	-0.32±0.22
Fornax:	+0.45±0.16	+0.25±0.12

the ‘standard’ versus ‘improved’ treatment of galaxy structure and dynamics.) The best fitting planes, under this minimisation scheme, are given in Table 6, as are the rms residuals of the data projected along the $\log R$ axis.

In order to use the methods in Feigelson & Babu (1992), these 3-dimensional data sets have been reduced to 2-dimensions by combining the distance-independent variables $\log \sigma$ and Σ . These were combined in such a way as to preserve the previously obtained optimal linear regression solution. This meant computing the ‘mixing’ value $b = -B/(2.5A)$, where A and B are the FP exponents given in Table 6, giving the quantity $\log \sigma + b \langle \mu \rangle$, where $\langle \mu \rangle$ is the mean surface brightness in mag units.[‡] A further linear regression calculation was performed, minimising the $\log R$ residuals at the expense of the $(\log \sigma + b \langle \mu \rangle)$ residuals. The code SLOPES, discussed in Isobe et al. (1990), was used to do this, and the results are presented in Table 7. As expected, due to the choice of the mixing value, the asymptotic formula gave the same slope as derived with the previous treatment of the FP variables in 3-dimensions. The slopes obtained with bootstrap and jackknife sampling are seen to vary slightly and have different associated uncertainties, as expected for small sample sizes. The errors from the bootstrapping procedure for the Fornax data set have been restricted as discussed previously.

The two techniques described in Feigelson & Babu (1992) for estimating the offset of parallel data sets have both been implemented here. These methods are subject to the condition that the Virgo and Fornax elliptical galaxy population define FPs which are parallel to each other. Given the uncertainties on the derived FP slopes (Table 7),

[‡] Σ is the mean surface brightness in linear units.

the Fornax cluster data does indeed define a plane which is consistent with being parallel to the Virgo cluster data. This is true when $R^{1/4}$ model parameters and CVD’s are used, and also when $R^{1/n}$ model parameters and infinite aperture velocity dispersions are used to construct the FP.

In the following method of analysis, a linear regression is performed on one of the cluster data sets, and the resulting regression line from this *calibration* is then applied to the second (parallel) cluster. One technique for measuring the intercept offset between parallel data sets was pioneered by Working & Hotelling (1929) and further developed by Feigelson & Babu (1992) to permit the x -values (i.e. distance-independent values) to be random variables rather than fixed quantities. With this method, the calibrated regression line for Virgo was applied individually to the data points in Fornax and a weighted mean offset attained; the method is discussed in Section 3.2 of Feigelson & Babu (1992) and their Appendix A2. This procedure encompasses the fact that the confidence intervals about the y -value one is trying to predict, given its x -value, will be larger for those data points at the ends of the distribution. This is because the uncertainty in the slope of the calibration line/plane gives greater freedom of movement to the calibration line at the ends of the distribution than in the center. This method of analysis gave an intercept offset, along the $\log R$ axis between the FP’s defined by the Virgo and Fornax data sets, of $\Delta \log R = -0.092 \pm 0.045$ dex and -0.064 ± 0.043 dex for the $(R^{1/4}, \sigma_0)$ parameters and the $(R^{1/n}, \sigma_{\text{tot},n})$ parameters, respectively.

In a similar fashion, the Fornax cluster has been used as the calibration sample, where the fitted regression line for Fornax is applied to the Virgo cluster. This was done with the Working-Hotelling confidence bands. Using the ‘standard’ FP parameters $(\sigma_0, R_{e,4}, \Sigma_{e,4})$, an intercept offset of $+0.091 \pm 0.031$ dex was computed. Using the ‘improved’ FP parameters $(\sigma_{\text{tot},n}, R_{e,n}, \Sigma_{e,n})$, an intercept offset of $+0.051 \pm 0.025$ dex was computed. These intercept offsets translate into a distance modulus of $+0.45 \pm 0.16$ mag (using $R^{1/4}$ model parameters and σ_0) and $+0.25 \pm 0.12$ mag (using $R^{1/n}$ model parameters and $\sigma_{\text{tot},n}$). The former estimate placing Fornax some $(23 \pm 8)\%$ further away than the Virgo cluster, compared to the latter estimate of $(12 \pm 6)\%$. These solutions are fully consistent with those obtained using the Virgo cluster as the calibration sample (see Table 8).

An alternative approach for computing the offset of parallel data sets was achieved following the methods in Section 3.1 of Feigelson & Babu (1992) and their Appendix A1. The FP data set from the Virgo cluster of galaxies was used to calibrate the *regression line* which was then applied to the FP data set of the Fornax cluster as a whole (and *vice-versa*). This was done in order to derive the intercept offset, along the $\log R$ axis, between the FP’s defined by the Virgo and Fornax clusters. The solutions obtained were similar, within 0.001 dex, to those calculated using the Working-Hotelling confidence bands, although the associated uncertainties were generally equal or larger. This served as a useful consistency check on the determination of the cluster-cluster distance modulus.

With the Working-Hotelling confidence bands, the uncertainty on the intercept offset, and hence the distance estimate, is reduced by the square-root of the sample size one is applying the calibrated solution to. Consequently, apply-

Table 7. Ordinary least-squares regression analysis for $\log R_e$ versus $(\log \sigma + b\Sigma_e)$, using the program SLOPES (Feigelson & Babu 1992). In each case, the value of $b = -B/(2.5A)$ is derived from the best fitting plane shown in Table 6.

method	Asymptotic Formula Slope (A)	Bootstrap Slope (A)	Jackknife Slope (A)
Virgo, $R^{1/4}[\sigma_0]$: $b=0.21$	1.11±0.08	1.10±0.08	1.11±0.09
Fornax, $R^{1/4}[\sigma_0]$: $b=0.21$	1.14±0.27	1.21±0.45	1.14±0.38
Virgo, $R^{1/n}[\sigma_{\text{tot},n}]$: $b=0.18$	1.62±0.09	1.62±0.09	1.62±0.10
Fornax, $R^{1/n}[\sigma_{\text{tot},n}]$: $b=0.22$	1.47±0.38	1.40±0.79	1.41±0.75

ing the Fornax *regression* line to Virgo, with a sample size of 18, results in a more accurate solution than achieved by applying the Virgo *regression* line to Fornax, with a sample size of only 7. However, this effect does have to compete with the fact that the uncertainty on the regression line is larger for a smaller calibration sample. As the generalised Working-Hotelling confidence bands propagate the errors in the calibrated line, this effect cannot be avoided, and the size of these errors influence the associated errors for the intercept offset. The lack of symmetry for the error estimates when using Virgo or Fornax as the calibrator is due to following: The error estimates on the slope of the regression line, which were propagated in the above analysis, were derived from the analytical expression for these terms. However, the errors on the slope and intercept will be under-estimated by the analytical expressions when the number of data points is small. This is seen in the FP solutions shown in Table 7, where the jackknife and bootstrapping methods of analysis provide a better estimate of the true size of these errors. Consequently, the error estimates on the previously given distance moduli should be multiplied by approximately the ratio of the bootstrapping error (or jackknife error if this is larger) to the asymptotic error (Feigelson & Babu 1992).

In addition, it should be noted that the FP slope uncertainties in Table 7 were estimated when the mixing value, b , was held fixed and assumed to have zero error. It should be remembered that it is the offset between two parallel planes, not two parallel lines, that is being measured. In order to fully estimate the uncertainties on the derived distance modulus, one must allow for errors in the optimal FP slopes for all axes. In so doing, one should return to the bootstrapping errors obtained with the 3-dimensional data set (Table 6). Working in 3-dimensions, the errors associated with the FP exponent A , are obtained by also letting the exponent B (and hence b) vary, as permitted by the bootstrapping analysis of the data. Therefore, the error obtained in the 3-dimensional analysis represents the true error estimate of the exponent A . Allowing for this, the errors to the solution for the Virgo-Fornax distance modulus are again multiplied by the ratio of the 3-D bootstrapping errors to the 2-D asymptotic errors. This procedure does not effect the optimal solution, only the associated uncertainties. The resulting solutions place Fornax (23±44)% ($R^{1/4}, \sigma_0$), and (12±36)% ($R^{1/n}, \sigma_{\text{tot},n}$) further away than Virgo.

5 DISCUSSION

In the interest of statistical completeness, galaxies with a CVD of less than 100 km s⁻¹ were not explicitly removed from the analysis. Due to the greater scatter in the FP below this value, past studies have enforced this arbitrary cut-off in their galaxy sample. However, it seems plausible to attribute the higher level of scatter to an inadequate treatment of the kinetic energy for these galaxies. As this is an issue which is addressed in this study, it made sense to leave these galaxies in the analysis.

Contributions from rotational energy to the total kinetic energy of a galaxy can in principle influence the slope of the FP. Djorgovski & Santiago (1993) noted that gains from including a rotational energy measurement would be offset by the introduction of additional measurement errors. Indeed, a marginal effect has been reported many times (Simien & Prugniel 1992; Busarello, Longo & Feoli 1992; Prugniel & Simien 1994). An asymmetric trend between the galaxy FP residuals and their maximum rotational velocity has also been found by D’Onofrio et al. (1996). More quantitative estimates from Prugniel & Simien (1996a,b), using a sample of 400 galaxies, claim that rotation can account for 25±15% of the departure of the FP from the virial expectation. While this figure may be true for FP’s constructed using early-type galaxies (E and S0), which includes almost all FP’s constructed to date, this figure can be reduced by the exclusion of S0 galaxies, known to have rotating disks. This was hinted at in the study by Busarello et al. (1997), who used only *bona fide* ellipticals to obtain a contribution of 15±28% to the tilt to the FP due to galaxy rotational energies.

In this paper, the FP was constructed using a culled set of galaxies, removing the S0s and keeping the Es. Contributions from possible rotational support to the kinetic energy term are expected to be minimal in this study of the FP. Four of the nine S0 galaxies which were excluded did actually have CVD’s less than 100 km s⁻¹, leaving only one galaxy in the remaining sample of 25 ellipticals with a CVD less than 100 km s⁻¹. It may indeed be that the increased scatter observed for the FP at the low velocity dispersion end is due to the presence of S0 galaxies that harbour rotating disks with significant rotational energies that are simply not measured through CVD measurements. For the Virgo cluster, exclusion of these objects resulted in a reduction of some 15-35% in the scatter about the FP, as evidenced by the rms residuals listed in Table 2 and Table 3.

For the Virgo cluster, exclusion of the S0's caused the final FP solution (incorporating the observed range of galaxy profiles and implied dynamics) to change from $R_{e,n} \propto \sigma_{tot,n}^{1.37 \pm 0.16} \Sigma_{e,n}^{-0.76 \pm 0.05}$ to $R_{e,n} \propto \sigma_{tot,n}^{1.72 \pm 0.24} \Sigma_{e,n}^{-0.74 \pm 0.09}$. This suggests that the inclusion of the S0 population not only increases the scatter about the FP (see Tables 2 and 3) but is also partly responsible for the departure of the FP from the relation $R \propto \sigma^2 \Sigma^{-1}$, predicted by the virial theorem. This is again easily understood as due to the neglect of rotational energies in the construction of the observed FP. It is therefore suggested that in addition to treating broken structural and dynamical homology, the construction of the FP always adopt the procedure of only using *bona fide* elliptical galaxies, unless one allows for rotational energies.

It is found that by addressing the range of structural and dynamical profiles evident amongst the elliptical galaxy population, the departure of the FP from the plane predicted by the virial theorem is reduced, confirming the results in Paper I. In addition, the scatter of the data points about the FP is reduced by some 20% for the sample of Fornax ellipticals and by the same amount for the sample of Virgo E and S0 galaxies. For the sample of Virgo ellipticals, the mean rms scatter about the FP is reduced by 40% after treating the range of galaxy structures and dynamics. This is evident in Tables 2, 3 and 4, which give the best fitting FP relation when one does and does not treat broken structural homology, and when one does and does not consistently measure the kinetic energy of the galaxies (i.e. uses σ_{tot} or CVD's, respectively). The first row of these 3 tables gives the FP which was constructed assuming that all galaxies are described by an $R^{1/4}$ profile and uses CVD's to represent the kinetic energy of each galaxy; This procedure gives the greatest departures of the FP from the virial plane. The final row in each Table gives the FP that was constructed allowing for a range of structural profiles amongst the galaxies, as described by the $R^{1/n}$ model, and measures the kinetic energy of each galaxy in a consistent manner by using the computed velocity dispersion within an aperture of infinite radius; This procedure gives the closest agreement between the FP and the virial plane. In fact, the formal solution for the FP of the Fornax cluster ($R_{e,n} \propto \sigma_{tot,n}^{2.03 \pm 0.78} \Sigma_{e,n}^{-1.07 \pm 0.30}$) is found to be in very close agreement with the prediction of the virial theorem, but does have large uncertainties associated with it because of the small number (7) of Fornax elliptical galaxies in the sample. Overall, it is concluded that addressing the range of structural profiles amongst the elliptical galaxies and better treating the galaxy dynamics reduces both the departure of the FP from the virial plane and the scatter about the FP.

In Paper I the Sersic light profile model was fitted to a sample of 26 E/S0 Virgo galaxies using the aperture magnitude profile data from Bower et al. (1992). Of these, 18 galaxies are in common with the sample of 25 used here. Comparison between the galaxy model parameters obtained in each study is not straight-forward, however. The galaxy profile data used here is in the form of surface brightness measurements along the major-axis, where as Paper I uses circular aperture magnitudes. Consequently, the models fitted in Paper I are more heavily weighted by the inner profile, and by necessity incorporate the central parts of the galaxy light. By contrast, the treatment of the surface brightness profiles here gives all data points along the profile equal

weight, and does not fit the central portion of the profile. In addition, the use of aperture magnitude data samples light from all position angles, and in so doing represents a mean light distribution for the galaxy as a whole. The presence of ellipticity gradients will result in the major- and minor-axis light profiles being described by different shape parameters so that $n_{maj} \neq n_{min}$. This is clearly evident in the range of shape parameters, n , for the major- and minor-axis, shown in the study of the Virgo ellipticals by Caon et al. (1993). Consequently, the mean light distribution obtained through the use of circular aperture magnitudes should not be expected to be identical to the light distribution along the major-axis. Finally, the data of Bower et al. (1992) was taken in the V-band, and that of Caon et al. (1993) in the B-band. Possible colour gradients, although expected to be small, may also contribute to differing results.

Despite the above factors, there is still fair agreement between the Sersic model parameters obtained using the different data sets. Galaxy scale-size and light profile shape for those galaxies in common between this Paper and Paper I are displayed in Figure 3. For comparison between the data sets, the Sersic model was fitted to the same radial extent ($<40''$) for each data set. This outer radius cut-off comes from the aperture magnitude profile limit of Bower et al. (1992), and has been applied, for this comparison, to the major-axis profiles of Caon et al. (1994). The correlation seen between the shape parameters has a linear correlation coefficient of 0.55, which increases to 0.82 upon removal of the 3 more discrepant points that are labeled in Figure 3. The correlation coefficient between the effective half-light radii is stronger at 0.93, suggesting that the range of galaxy sizes, and structures, can be *largely* reproduced from both types of observational data. The galaxies which appear to have the more discrepant shape parameters are the flattened S0 galaxy NGC 4550, NGC 4486, and NGC 4564 which has a value of $n=4.64$ (Paper I) lying between $n_{maj}=1.51$ and $n_{min}=5.08$ (Caon et al. 1993) and is therefore not a discrepant point after all.

Despite the above differences, it is interesting to compare the resulting FP's obtained using the independent data sets. Firstly, assuming structural homology and using $R^{1/4}$ model parameters and CVD measurements for the Virgo cluster of galaxies, the FP was found in Paper I to be described by $R_{e,4} \propto \sigma_0^{1.33 \pm 0.10} \Sigma_{e,4}^{-0.79 \pm 0.11}$. This is to be compared with $R_{e,4} \propto \sigma_0^{1.10 \pm 0.14} \Sigma_{e,4}^{-0.55 \pm 0.09}$ found in this study. The exponents on the velocity dispersion term are consistent within the 1σ joint errors, and the exponents on the surface brightness term are consistent within the 2σ joint errors. Allowing for broken structural homology and consistently measuring the velocity dispersion within an aperture of infinite radius, it was found in Paper I that the FP for Virgo is described by $R_{e,n} \propto \sigma_{tot,n}^{1.44 \pm 0.11} \Sigma_{e,n}^{-0.93 \pm 0.08}$. This should be compared with $R_{e,n} \propto \sigma_{tot,n}^{1.37 \pm 0.16} \Sigma_{e,4}^{-0.76 \pm 0.05}$. The relative consistency between the exponents is the same as before. It is noted that the uncertainties on the FP exponents are based upon the statistics of the linear regression to the data points; they do not incorporate possible measurement errors in the data points themselves. It is also noted that the sample of Virgo galaxies used in Paper I contains 7 galaxies that this study does not include, and this study also contains 7 galaxies not present in the sam-

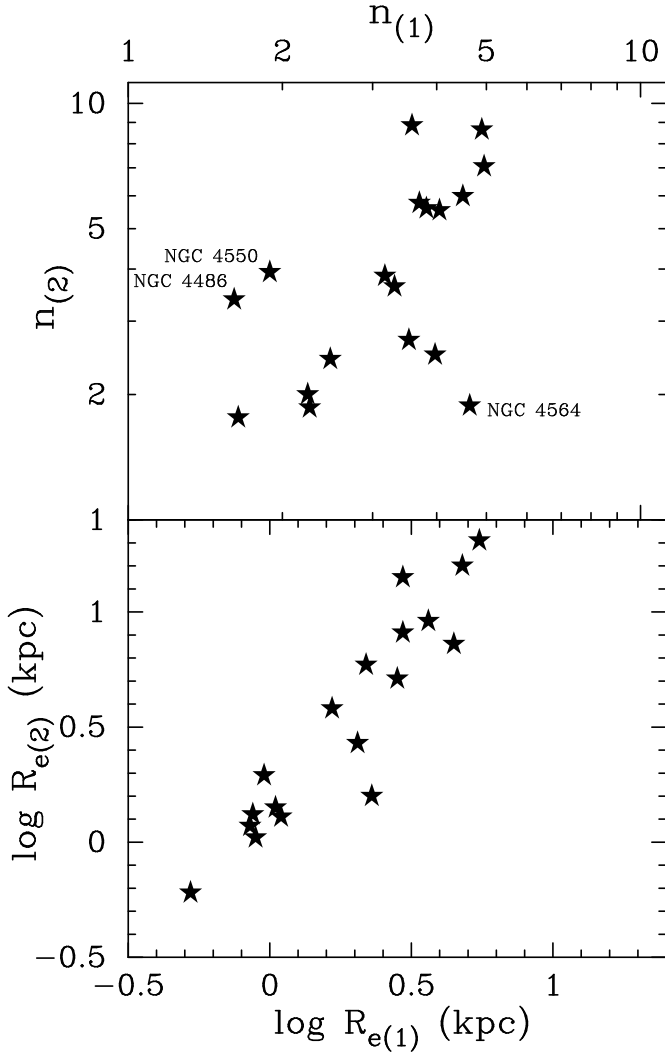


Figure 3. The Sersic $R^{1/n}$ model parameters for the effective radius, R_e , and shape parameter, n , are displayed for 18 galaxies from Paper I which are in common with the sample in this study. The subscript (1) denotes that the parameters were obtained from Paper I, and the subscript (2) refers to the values obtained in this study.

ple of Paper I. Using only those 18 galaxies in common, the resulting FP's were found to be in acceptable agreement with each other, with the FP described by the data in Paper I given by the relation $R_{e,n} \propto \sigma_{\text{tot},n}^{1.29 \pm 0.10} \Sigma_{e,n}^{-0.89 \pm 0.05}$, and that obtained using this study's data given by the relation $R_{e,n} \propto \sigma_{\text{tot},n}^{1.26 \pm 0.12} \Sigma_{e,n}^{-0.81 \pm 0.04}$. The main point is that both studies show that by treating the range of luminosity and dynamical structures inherent amongst the early type galaxies the departure of the FP from the virial plane is reduced.

D'Onofrio et al. (1996) also constructed a FP for the Virgo and Fornax clusters using the data of Caon et al. (1994). The approach taken in this study differs in several ways to that of D'Onofrio et al. (1996). This work has used model-determined effective radii and the model-determined mean surface brightness within these radii, where as D'Onofrio et al. (1996) used model-independent values for these quantities (Caon et al. 1994). The model-determined quantities are those derived from the $R^{1/n}$ model

fitted to the undisturbed portion the galaxy light profile. This portion is free from any peculiarities of the inner light profiles (noted by Caon et al. 1993), is not heavily distorted by the presence of a disk or dust lanes, and is uncontaminated from possible tidal interactions which may have perturbed the original galaxy profile, particularly in the outer parts. The parameters used by D'Onofrio et al. (1996) are better estimates of the half-light radii, in the true sense of the term, in that they are the radii which enclose half of the total light from the galaxy, although the total light was derived by extrapolating the observational data to $\mu_B=32$ with $R^{1/4}$ profiles (Caon et al. 1994). The preferred dynamical term used here differs from that used by D'Onofrio et al. (1996). While they used CVD values, this paper has also used, and in fact prefers, the infinite aperture velocity dispersion derived from the application of the Jeans equation (Ciotti 1991; Paper 1). D'Onofrio et al. (1996) gave their Virgo FP solution as $R_{e,n} \propto \sigma_0^{1.26 \pm 0.09} \Sigma_{e,n}^{-0.70 \pm 0.03}$. This is in good agreement with the FP solution derived here, which addressed the range of structural profiles but used CVD measurements. For the sample of Virgo E and S0 galaxies the relation $R_{e,n} \propto \sigma_0^{1.12 \pm 0.17} \Sigma_{e,n}^{-0.64 \pm 0.07}$ was obtained here.

D'Onofrio et al. (1996) computed a Virgo-Fornax distance modulus of 0.50 mag (using the FP) and 0.45 ± 0.15 mag (using the D_n - σ relation). This result is in close agreement with the distance modulus derived in this study based upon galaxy parameters from the $R^{1/4}$ profile and using CVD's, where a value of 0.45 ± 0.16 mag (asymptotic error) was computed. Using $R^{1/n}$ model parameters and infinite aperture velocity dispersion measurements, however, this study found the Virgo-Fornax distance modulus to be 0.25 ± 0.12 mag (asymptotic error). Given that D'Onofrio et al. (1996) allowed for different galaxy structures through using model-independent estimates of the half-light radius and associated mean surface brightness, but used CVD's, the final estimate of 0.25 mag appears to be different because of the treatment of the dynamical term rather than the treatment of the structural quantities. Indeed, D'Onofrio et al. (1997) introduced their own aperture correction to the velocity dispersion term, finding a reduced Virgo-Fornax distance modulus of 0.30 ± 0.05 mag (formal error).

Comparison with other methods of distance determination yields good agreement with the distance modulus of $+0.25 \pm 0.12$ mag obtained in Section 4. The investigation by McMillan et al. (1993), using the planetary nebula luminosity function, found a Virgo-Fornax distance modulus of $+0.24 \pm 0.10$ mag. Another accurate estimate has been derived using the method of surface brightness fluctuations, where a value of 0.20 ± 0.08 mag has been obtained (Tonry et al. 1997). Using a sample of E and S0 galaxies, Dressler et al. (1987) applied the D_n - σ relation to compute a value of $+0.14 \pm 0.18$ mag. An alternate approach using type Ia supernovae (Hamuy et al. 1991) found a yet lower value of 0.09 ± 0.14 mag, although still consistent within the errors of the value derived here.

However the result presented here is in poorer agreement with studies using the globular cluster luminosity function (-0.5 ± 0.2 mag, Bridges, Hanes & Harris 1991) and with studies which have used the Tully Fisher (TF) relation for spiral galaxies. The H-band TF relation used by Aaronson et al. (1989) placed the Fornax cluster closer than Virgo, giving a distance modulus of -0.25 ± 0.23 mag for Fornax rel-

ative to Virgo. More recently, Bureau et al. (1996) used an I-band TF relation. Demanding equal slopes for the TF relation in each cluster, and allowing for errors on both axes, they obtained a value of -0.04 ± 0.15 mag. This result is not as inconsistent with the analysis in this paper as one might first think. It should be noted that the bootstrapping error analysis, performed in Section 4, revealed that the estimate of the error based upon analytical asymptotic expressions was too small due to the small sample size (see Table 7). Correction for this increased the error estimate from 0.12 mag to 0.27 mag. The treatment in Bureau et al. (1996), and indeed most papers of this kind, has similarly underestimated the true size of their errors for the same reason – the analytical expression for the size of the errors underestimates the true size of the errors when the sample size is small (approximately <50). In addition, it is known that spiral galaxies are less centrally concentrated within a cluster than the elliptical galaxies, so they may not provide as accurate a measurement of the cluster distance as the ellipticals can. This could be particularly relevant for Virgo, a cluster known to have a considerable line-of-sight depth (Tonry, Ajhar & Luppino 1990; Jacoby et al. 1992).

The Virgo-Fornax distance modulus obtained in this paper is also only marginally consistent with the study by Bothun, Caldwell & Schombert (1989) who used the surface brightness profiles of dwarf ellipticals to compute a distance modulus of -0.16 ± 0.16 mag. By the nature of their study, they also sampled a different galaxy population than used here, which again may partly explain the disagreement in distance modulus. It is also observed that they made no mention of having used any numerical resampling technique to estimate the size of their errors. To extrapolate, this opens up the possibility that many past inconsistencies between cluster distance estimations may be simply due to an inadequate, and under-estimation, of the associated errors.

There are other effects which have been proposed to influence the tilt of the FP. One of these is orbital anisotropy in the galaxies' internal velocity fields. This has been explored in detail in the studies by Ciotti, Lanzoni & Renzini (1996) and Ciotti & Lanzoni (1997). Using the Jeans equation, they performed theoretical modeling of the dynamics of a range of $R^{1/n}$ surface brightness profiles ($n=1-10$), and for the Hernquist (1990) and Jaffe (1983) density models. They explored possible variations in the orbital anisotropy with radius. Rejecting those models which are likely to be unstable, they found that variations to the tilt of the FP due to orbital anisotropy are confined within the known thickness of the FP and can thus have no significant influence on the FP tilt.

The influence of differing stellar populations, as given by line strength indices such as Mg_2 or broad band colours such as B-V, was initially determined to have little or no effect on the slope of the FP (Djorgovski & Davis 1987; Lynden-Bell et al. 1988; Jørgensen et al. 1993). However, more recent estimates of the influence from differing stellar metallicities and ages are suggesting a greater effect on the slope of the FP (Gregg 1992; Guzman & Lucey 1993). Prugniel & Simien (1996a,b) combined four broad band colours and the Mg_2 index in the extraction and computation of a mean measure of the influence of differing stellar populations. They found that stellar populations may account for half of the observed tilt to the FP. If confirmed, this would

easily explain any remaining tilt to the FP, and may place one in the unexpected position of having the FP tilt the other way.

6 SUMMARY

For a sample of Virgo and Fornax early-type galaxies, the surface brightness profiles from Caon et al. (1994), which are known to represent a range of luminosity structures, have been used to explore the tilt and thickness of the FP. This study also explores the range of luminosity structures present amongst the early-type galaxies using the Sersic $R^{1/n}$ model rather than forcing structural homology through use of the $R^{1/4}$ model (see also Caon et al. 1993). The $R^{1/n}$ light profile model has been used to parameterise the size (as given by the effective radius $R_{e,n}$) and mean surface brightness ($\Sigma_{e,n}$) for each galaxy. Solving the Jeans equation, the associated range of dynamical structures has been computed and the projected velocity dispersion within an aperture of infinite radius ($=1/3$ of the virial velocity dispersion; Ciotti 1994) has been derived. This approach measures the velocity dispersion of each galaxy in a consistent fashion. CVD measurements sample different fractions of different galaxy's dynamical profiles, where as the infinite aperture velocity dispersion consistently measures galaxies in the same way, and therefore provides a better estimate of a galaxy's kinetic energy.

The trend of increasing shape parameter n with increasing values of the model-independent half-light radius (Caon et al. 1993), is also shown to be present when using the $R^{1/n}$ model-determined effective radius $R_{e,n}$. A χ^2 error analysis of the fitted model parameters shows that this is not due to coupling between the model parameters implying it is a real physical relation. A principal component analysis reveals that greater than 97% of the variance in the FP data set (σ, R, Σ) resides within 2 dimensions, confirming the appropriateness of fitting a plane to this data.

It is concluded that broken structural and dynamical homology are responsible, at least in part, for the departure of the FP from the relation $R \propto \sigma^2 \Sigma^{-1}$ predicted by the virial theorem. Having used an independent set of data obtained by different observers with a different instrument and reduction procedures, this confirms the results of Paper I. This conclusion is supported by the additional analysis of the Fornax cluster.

For comparison of the the FP with the virial theorem, the FP was constructed using the bisector method of linear regression in 3 dimensions. Due to the small galaxy sample size, a bootstrapping procedure was employed to estimate the uncertainty on the FP slope. Using a sample of 25 Virgo E (18) and S0 (7) galaxies, the FP constructed using $R^{1/4}$ model parameters and CVD measurements was found to be given by the relation $R_{e,4} \propto \sigma_0^{1.10 \pm 0.14} \Sigma_{e,4}^{-0.55 \pm 0.09}$. Allowing for broken structural and broken dynamical homology, this plane was observed to change to $R_{e,n} \propto \sigma_{tot,n}^{1.37 \pm 0.16} \Sigma_{e,n}^{-0.76 \pm 0.05}$. The perpendicular rms scatter about these FP's is 0.099 to 0.077 dex respectively.

Given that the S0 galaxies likely possess significant rotational energy that is not dealt with through use of velocity dispersion measurements, they were removed from the sample of Virgo galaxies and the above anal-

ysis was re-performed. The resulting FP was found to change from $R_{e,4} \propto \sigma_0^{1.19 \pm 0.21} \Sigma_{e,4}^{-0.60 \pm 0.11}$ to $R_{e,n} \propto \sigma_{\text{tot},n}^{1.72 \pm 0.24} \Sigma_{e,n}^{-0.74 \pm 0.09}$. The perpendicular rms scatter to the plane was found to decrease by 40% from 0.084 to 0.050 with the fuller treatment of galaxy structure and dynamics.

The FP for a sample of 7 elliptical galaxies in the Fornax cluster, was also computed under the same conditions as above. The Fornax FP was found to change from $R_{e,4} \propto \sigma_0^{1.69 \pm 0.83} \Sigma_{e,4}^{-0.85 \pm 0.30}$ to $R_{e,n} \propto \sigma_{\text{tot},n}^{2.03 \pm 0.78} \Sigma_{e,n}^{-1.07 \pm 0.30}$, with perpendicular rms scatter of 0.064 and 0.050 respectively. The formal solution of the latter FP is in close agreement with the plane predicted by the virial theorem, and it will be of interest to see how/if this solution changes for a larger sample of galaxies.

Constructing the Virgo FP by minimising the residuals of the $\log R$ variable and applying this to the Fornax data, through use of the improved Working-Hotelling confidence bands approach developed by Feigelson & Babu (1992), enabled an estimation of the relative distance between the two clusters. Forcing structural homology (i.e. fitting $R^{1/4}$ profiles) and using CVD's, a Virgo-Fornax distance modulus of 0.46 ± 0.16 mag (analytical error) was obtained. Allowing for the range of galaxy structures observed in the data, and using the infinite aperture velocity dispersion, the Virgo-Fornax distance modulus was computed to be 0.25 ± 0.12 mag (analytical error). A fuller estimate of the associated uncertainties to these distance moduli was achieved through a numerical resampling of the 3-dimensional FP data set. This analysis made the Fornax cluster (23 ± 44)% and (12 ± 36)% more distant than the Virgo cluster, for the respective models above.

Acknowledgments

I thank Mauro D'Onofrio for making his galaxy profile data available to me in electronic form. I also thank Eric Feigelson and Ron Kollgaard for providing me with their computer codes to compute the intercept offset between parallel data sets, and for their quick help with my queries. I am also grateful for the use of Eric Feigelson's computer code SLOPES. I thank Matthew Colless for his proof reading of this manuscript and his useful suggestions. This research has made use of the NASA/IPAC Extragalactic Database (NED) which is operated by the Jet Propulsion Laboratory, California Institute of Technology, under contract with the National Aeronautics and Space Administration.

REFERENCES

- Aaronson M. et al., 1989, ApJ, 338, 654
 Bender R., Saglia R.P., Gerhard O.E., 1994, MNRAS, 269, 785
 Bevington P.R., 1969, Data Reduction and Error Analysis for the Physical Sciences. New York, McGraw-Hill
 Binggeli B., Cameron L.M., 1991, A&A, 252, 27
 Bothun G.D., Caldwell N., Schombert J.M., 1989, AJ, 98, 1542
 Bower R.G., Lucey J.R., Ellis R.S., 1992, MNRAS, 254, 589
 Bridges T.J., Hanes D.A., Harris, W.E., 1991, AJ, 101, 469
 Bureau M., Mould J.R., Staveley-Smith, L., 1996, ApJ, 463, 60
 Burstein D., Heiles C., 1978, ApJ, 225, 40
 Burstein D., Heiles C., 1984, ApJS, 54, 33
 Burstein D., Davies R.L., Dressler A., Faber S.M., Stone R.P.S., Lynden-Bell D., Terlevich R.J., Wegner G., 1987, ApJS, 64, 601
 Busarello G., Longo G., Feoli A., 1992, A&A, 262, 52
 Busarello G., Capaccioli M., Capozziello S., Longo G., Puddu E., 1997, A&A, 320, 415
 Caon N., Capaccioli M., D'Onofrio M., 1993, MNRAS, 265, 1013
 Caon N., Capaccioli M., D'Onofrio M., 1994, A&AS, 106, 199
 Capaccioli M., 1989, in Corwin H.G., Bottinelli L., eds, The World of Galaxies. Springer-Verlag, Berlin, p.208
 Capaccioli M., Caon N., 1989, in Grobøl P.J., Murtagh F., Warmels R.H. eds., Proc. ESO/ST-ECF workshop on: Data Analysis. ESO, Garching, p. 107
 Capaccioli M., Longo G., 1994, A&A Review, 5, 293
 Ciotti L., 1991, A&A, 249, 99
 Ciotti L., 1994, Cel. Mech. & Dynam. Astr., 60, 401
 Ciotti L., Lanzoni B., 1997, A&A, 321, 724
 Ciotti L., Lanzoni B., Renzini A., 1996, MNRAS, 282, 1
 Davies R.L., Efstathiou G., Fall S.M., Illingworth G., Schecter P.L., 1983, ApJ, 266, 41
 de Vaucouleurs G., 1948, Ann d'Ap., 11, 247
 de Vaucouleurs G., 1953, MNRAS, 113, 134
 de Vaucouleurs G., de Vaucouleurs A., Corwin H.G.Jr., Buta R.J., Paturel G., Fouque P. 1991, in Third reference catalogue of bright galaxies. Springer-Verlag
 Djorgovski S., Davis M., 1987, ApJ, 313, 59
 Djorgovski S., Santiago B.X., 1993, in Danziger J. et al., eds, Proc. of the ESO/EIPC Workshop on Structure, Dynamics, and Chemical Evolution of Early-Type Galaxies. ESO Publication 45, p.59
 D'Onofrio M., Capaccioli M., Caon N., 1994, MNRAS, 271, 523
 D'Onofrio M., Capaccioli M., Zaggia, S.R., Caon N., 1997, MNRAS, in press
 D'Onofrio M., Longo G., Capaccioli M., 1996, in Buzzoni A., Renzini A., Serrano G., eds, ASP Conf. Ser. Vol. 86, Fresh views of elliptical galaxies. Astron. Soc. Pac., san Francisco, p. 143
 Dressler A., Lynden-Bell D., Burstein D., Davies R.L., Faber S.M., Terlevich R.J., Wegner G., 1987, ApJ, 313, 42
 Feigelson E.D., Babu G.J., 1992, ApJ, 397, 55
 Graham A., Colless M.M., 1997a, MNRAS, 287, 221, Paper I
 Graham A., Colless M.M., 1997b, in Arnaboldi M., Da Costa, G.S., Saha P., eds, ASP Conf. Ser. Vol. 116, The Second Stromlo Symposium – The Nature of Elliptical Galaxies. Astron. Soc. Pac., san Francisco, p. 175
 Graham A., Lauer T.R., Colless M., Postman M., 1996, ApJ, 465, 534
 Gregg M.D., 1992, ApJ, 384, 43
 Guzman R., Lucey J.R., 1993, MNRAS, 263 L47
 Hamuy M., Phillips M.M., Maza J., Wischnjewsky M., Uomoto A., Landolt A.U., Khatwani R., 1991, AJ, 102, 208
 Hernquist L., 1990, ApJ, 356, 359
 Illingworth G., 1983, in Athanassoula E., ed., Proc. IAU Symp. 100, Internal Kinematics and Dynamics of Galaxies. Kluwer, Dordrecht, p. 257
 Isobe T., Feigelson E.D., Akritas M.G., Babu G.J., 1990, ApJ, 364, 104
 Jacoby G.H. et al., 1992, in ??? eds, ASP Conf. Ser. Vol. 104, ??? Astron. Soc. Pac., san Francisco, p. 599
 Jaffe W., 1983, MNRAS, 202, 995
 Jørgensen I., Franx M., Kjærgaard P., 1993, ApJ, 411, 34
 Lynden-Bell D., Burstein D., Davies R.L., Dressler A., Faber S.M., Terlevich R., Wegner G., 1988a, in Pritchett C.J., Vandenberg S., eds, ASP Conf. Proc. 4, The Extragalactic Distance Scale, ASP, San Francisco, p.307
 McElroy D.B., 1995, ApJS, 100, 105
 McMillan R., Ciardullo R., Jacoby G.H., 1993, ApJ, 416, 62
 Michard R., 1985, A&AS, 59, 205
 Murtagh F., Heck A., 1987, Multivariate Data Analysis. Reidel, Dordrecht

- Prugniel Ph., Simien F., 1994, *A&A*, 281, L1
Prugniel Ph., Simien F., 1996a, *A&A*, 309, 749
Prugniel Ph., Simien F., 1996b, in Buzzoni A., Renzini A., Ser-
rano G., eds, *ASP Conf. Ser. Vol. 86, Fresh views of elliptical
galaxies*. Astron. Soc. Pac., san Francisco, p. 143
Schombert J.M., 1986, *ApJS*, 60, 603
Sersic J.-L., 1968, *Atlas de Galaxias Australes*, Observatorio As-
tronomico, Cordoba
Simien F., Prugniel Ph., 1992, in Longo G., Capaccioli M.,
Busarello G., eds, *Morphological and physical classification
of galaxies*. Kluwer, Dordrecht, p. 431
Tonry J.L., Ajhar E.A., Luppino G.A., 1990, *AJ*, 100, 1416
Tonry J.L., Blakeslee J.P., Ajhar E.A., Dressler A., 1997, *ApJ*,
475, 399
Working H., Hotelling H., 1929, *J. Am. Stat. Assoc. Suppl.*, 24 73